Available online at www.sciencedirect.com
ScienceDirect
Bioorganic & Medicinal Chemistry 16 (2008) 6207–6217
Bioorganic & Medicinal Chemistry

Identification of non-lipid LPA_3 antagonists by virtual screening

James I. Fells,[a] Ryoko Tsukahara,[b] Yuko Fujiwara,[b] Jianxiong Liu,[b] Donna H. Perygin,[a] Daniel A. Osborne,[a,b] Gabor Tigyi[b] and Abby L. Parrill[a,*]

[a]*Department of Chemistry and Computational Research on Materials Institute, The University of Memphis, Memphis, TN 38152, USA*
[b]*Department of Physiology, University of Tennessee Health Science Center, Memphis, TN 38163, USA*

Received 11 January 2008; revised 15 April 2008; accepted 16 April 2008
Available online 18 April 2008

Abstract—In the present study, we utilized virtual screening to identify LPA_3 antagonists. We have developed a three-point structure-based pharmacophore model based on known LPA_3 antagonists. This model was used to mine the NCI database. Docking, pharmacophore development, and database mining produced new, non-lipid leads. Experimental testing of seven computationally selected pharmacophore hits produced one potentiator and three antagonists, one of which displays both LPA_3 selectivity and nanomolar potency. Similarity searching in the ChemBridge database using the most promising lead as the search target produced four additional LPA_3 antagonists and a potent dual $LPA_{1\&2}$ antagonist.

1. Introduction

Lysophosphatidic acid (LPA) is a phospholipid mediator that elicits a host of biological effects including cell proliferation, survival, motility and differentiation.[1,2] LPA evokes many of these responses extracellularly through G protein-coupled receptors (GPCR) that belong either to the endothelial differentiation gene family: EDG2/LPA_1, EDG4/LPA_2, EDG7/LPA_3,[3] or to a subcluster in the purinergic GPCR family p2y9/LPA_4,[4] GPR92/LPA_5,[5] and GPR87/LPA_6.[6] LPA receptors are implicated in cardiovascular disease and atherosclerosis through their action on platelets, leukocytes, and the different cell types of the arterial wall.[7,8] LPA has been shown to regulate cancer cell invasion, metastasis, and resistance to both chemotherapeutics and radiation.[9,10] Due to these many therapeutically relevant effects of LPA, highly selective receptor antagonists are important, but not yet available. The specific role of the LPA receptors in these diseases is difficult to assess because many cells express combinations of LPA receptors.[1,2] Subtype-specific antagonists could also serve as important tools to elucidate the pathological and physiological roles elicited by a particular LPA subtype.

LPA_3 shows a limited expression pattern in the testes, prostate, pancreas, heart, lung, and ovary,[11–13] unlike LPA_1 or LPA_2, which are expressed in almost all tissues.[11] LPA and the LPA_3 receptor in particular is important in embryo implantation and uterine motility.[14] This restricted expression and the distinct biological functions make LPA_3 an attractive drug target for gynecological and reproductive diseases. Identification of selective LPA_3 antagonists in particular has the potential to contribute to studies of the role of LPA in cardiovascular disease and reproduction.

Several LPA receptor antagonists (Fig. 1) have been reported to date but all, with the exception of the non-selective Ki16425,[15] are lipids which do not satisfy Lipinsky's rule of five.[16] No single receptor-selective antagonists for any of the six LPA receptors have been reported. Ohta et al. showed that Ki16425 is a non-selective $LPA_{1/2/3}$ antagonist.[15] Ki16425 is an isoxazole derivative that has greater potency for LPA_3 than LPA_1 and LPA_2.[15] Fatty alcohol phosphates (FAP) with 12- and 14-carbon alkyl chains and the short-chain phosphatidic acid analogs, dioctylglycerol phosphate (DGP) and dioctylglycerol thiophosphate (DGTP), are selective for LPA_1 and LPA_3 over LPA_2.[17,18] DGP and DGTP have IC_{50} values of 143 and 184 nM, respectively, for the LPA_3 receptor and their IC_{50} values at the LPA_1 receptor are only 2- and 10-fold higher than for LPA_3. Although several additional LPA_3 antagonists have been reported,[17–20] (Fig. 1), their structures are closely

Keywords: Lysophosphatidic acid; GPCR; Database mining; Pharmacophore.
* Corresponding author. Tel.: +1 901 678 2638; fax: +1 901 678 3447; e-mail: aparrill@memphis.edu

0968-0896/$ - see front matter © 2008 Elsevier Ltd. All rights reserved.
doi:10.1016/j.bmc.2008.04.035

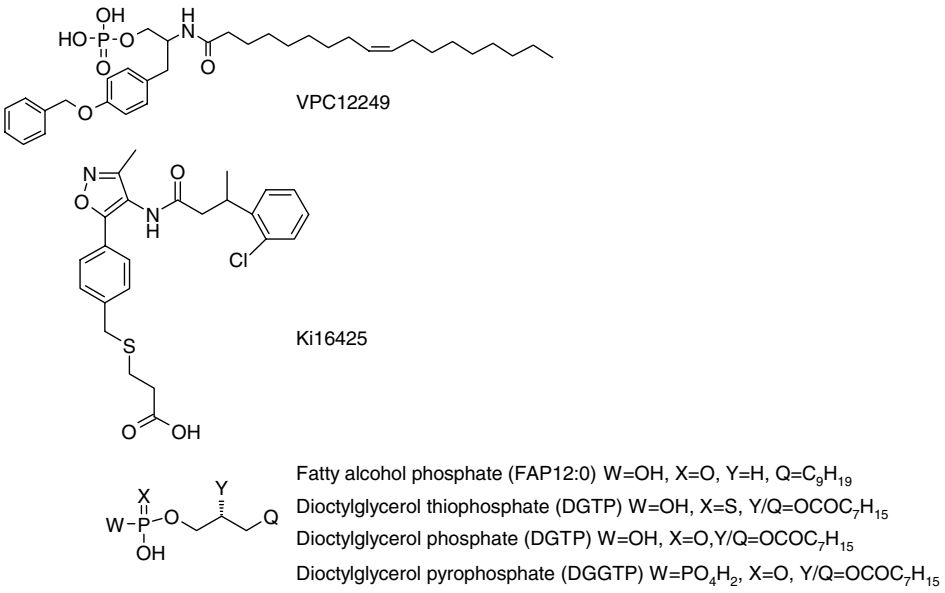

Figure 1. LPA receptor antagonist structures.

related to these lipid-like antagonists. Ki16425, DGP, and DGTP, therefore, represent the available diversity that defines the spatial arrangements of functional groups necessary for LPA_3 antagonist activity (the pharmacophore) and can potentially assist in identification of other, structurally unrelated, compounds.

The dual action of the presently known antagonists at both LPA_3 and LPA_1 suggests that information regarding the active conformation at the LPA_3 receptor is critical for successful pharmacophore development. Since no crystal structure of the LPA_3 receptor is currently available, such information at the present time can only come from modeling studies. We have modeled the LPA_{1-3} receptor structures and complexes with both agonists and antagonists.[21–23] Extensive computationally guided mutagenesis studies have confirmed key residues responsible for agonist binding.[24] Residues experimentally confirmed to be important for LPA recognition in LPA_3 using the nomenclature of Ballesteros and Weinstein[25] are Arg 3.28 and Glu 3.29, which are conserved in the LPA_{1-3} receptors, along with Lys 7.35 and Arg 5.38.[21]

In the present study pharmacophore development, database mining, and docking have been applied to identify subtype-specific, non-lipid LPA_3 antagonists. Based on the previous computational models of the LPA receptors[21,23,26] along with SAR data for known LPA antagonists,[15,17–20,27,28] we developed a structure-based pharmacophore. We pursued a structure-based approach to account for key interactions of the ligands with the LPA_3 receptor. This allowed definition of a pharmacophore specific to LPA_3 antagonism using the currently known antagonists even though they display dual activity at both LPA_1 and LPA_3. The resultant pharmacophore was used to search databases for potential antagonist leads. Rigid docking afforded us the capability to rapidly screen and further refine the hits generated from our database searching. Pharmacophore searching of the NCI database[29] and further hitlist refinement identified seven potential LPA_3 antagonists. Pharmacological assays were used to establish receptor selectivity. Pharmacological screening confirmed one LPA_3 potentiator and four LPA_3 antagonists with submicromolar K_i, one of which displays both LPA_3 selectivity and nanomolar potency. Single reference similarity searching in the ChemBridge database yielded five more LPA_3 receptor antagonists, and a full $LPA_{1\&2}$ antagonist. Here we report the first antagonist with receptor selectivity for LPA_3 over $LPA_{1/2/4/5}$.

2. Results

Docking simulations using the inactive LPA_3 model were performed with the three known LPA_3 antagonists, DGP, DGTP, and Ki16425. These studies provided insight into interactions that may be important for antagonist activity by comparing docking simulations of each antagonist in the LPA_3 receptor. Key residues predicted to interact with the ligands were R3.28, R7.36, K95, K7.35, and H5 (Fig. 2). In particular, docking studies suggested the anionic group of all three ligands ion paired with R7.36, K95, and R3.28 (Table 1). These data and prior studies suggest that the antagonists and agonists share interactions with R3.28 and R7.35.[21,23] These electrostatic interactions were deemed to be important for developing competitive antagonists.

A structure-based pharmacophore was generated from the superposition of these antagonists. The model takes into account interactions within 4.5 Å of the known antagonists, based on the expectation that these are critical for antagonistic activity. The LPA_3 antagonist pharmacophore is a three-point pharmacophore model consisting of an anionic group and two hydrophobic regions, shown in Figure 3. The anionic group is spaced 8–14 Å and 12–16 Å from the two hydrophobic regions. Hydrophobic regions are spaced 7–12 Å apart.

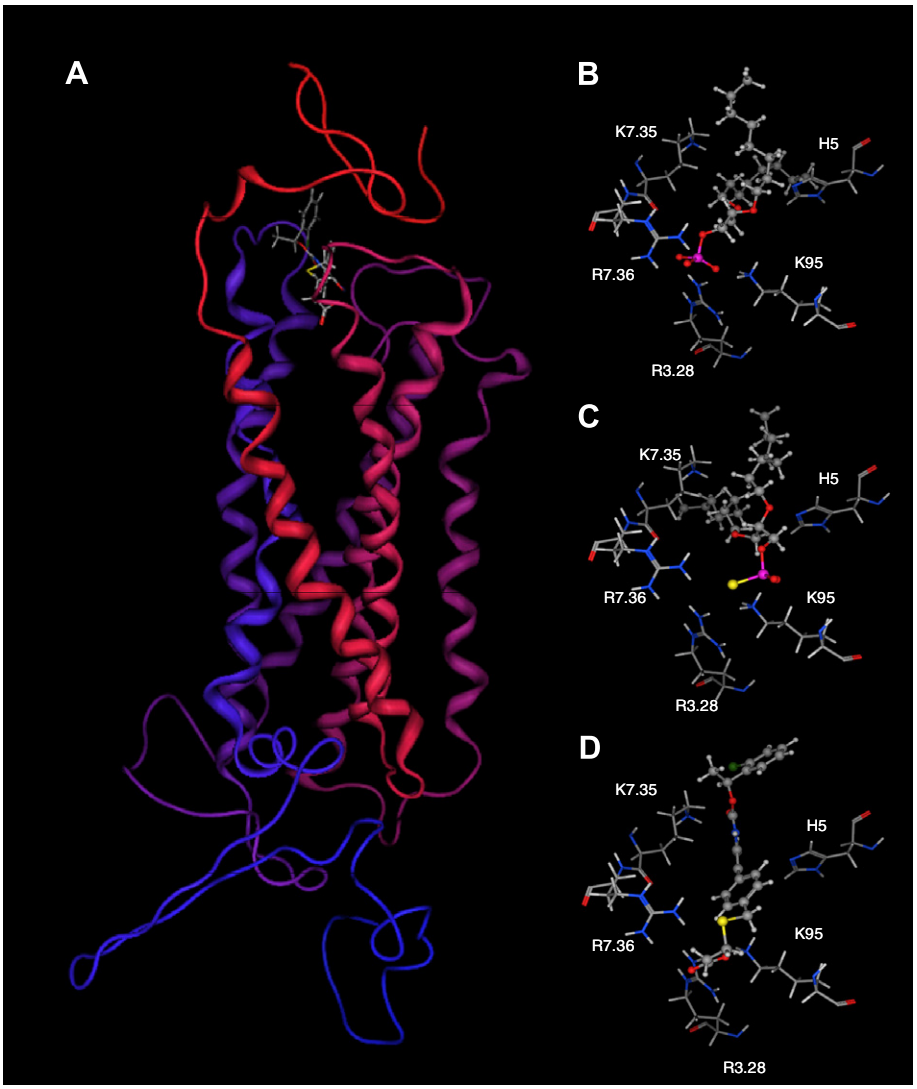

Figure 2. Models of LPA_3 receptor complexes with antagonists (Ki16425, DGTP, and DGP). Protein shown as ribbon with Ki16425 as a ball and stick model in (A). (B) (DGP), (C) (DGTP), and (D) (Ki16425), show antagonist (ball and stick) interactions with key amino acid residues (sticks) from a common perspective.

Table 1. Interaction distances (Å) between published antagonists and selected LPA_3 receptor residues

Compound	R3.28	K7.35	R7.36	W25	K95	H5	R267	W102	Y6	Total # of ionic/polar interactions
Ki16425	**2.50**	*4.26*	**4.38**	4.02	**2.46**	*3.78*		4.12	3.70	5
DGTP	**4.57**	3.15	**3.57**	3.67	**3.07**	3.01	4.26	*3.07*	4.23	4
DGP	**2.28**	4.25	**2.08**	2.84	**2.54**	3.43		*4.27*		4

Interactions with distances >4.5 Å are not included.
Ionic interactions identified by bold type.
Complementary polar interactions identified by italic type.
Hydrophobic interactions underlined.

The pharmacophore was used to mine the National Cancer Institute (NCI) Developmental Therapeutics Chemical Database. A search of this NCI database with various anionic functional groups (Table 2) identified 1098 hits. One of the hits included the known LPA_3 antagonist, dodecyl phosphate (FAP 12:0).[18] Many of the hits, including mesuprine, methotrexate, and *N*6-benzyladenosine-5′-phosphate (NBAP, Fig. 4) are structurally distinct from known antagonists, offering diversity in new candidate structures.

In silico screening was used to reduce the pharmacophore hits to the most promising compounds for pharmacological assay. Visual assessment prior to rigid docking was used to evaluate whether the compound was too large in size. This assessment slightly reduced the 1098 compound hit list.

One hit, NBAP, when tested experimentally did not show either an antagonist or agonist response, but acted as a potentiator when co-administered with LPA

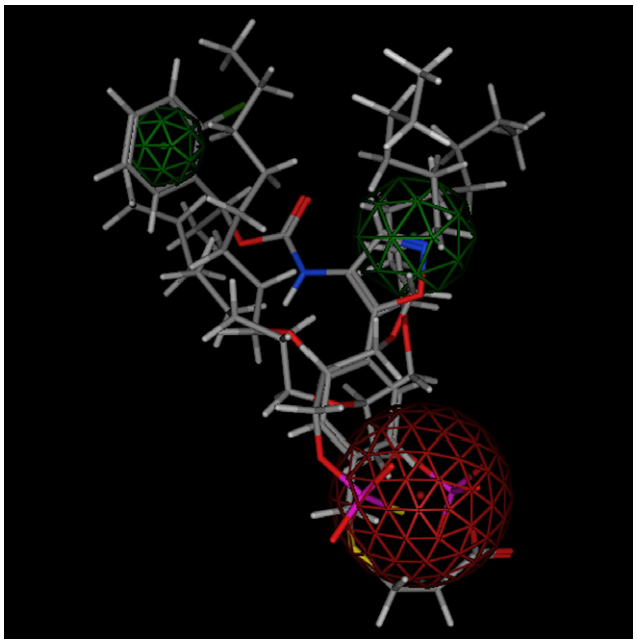

Figure 3. Superimposition of docked LPA_3 antagonists DGTP, DGP, and Ki16425 used to develop the LPA_3 antagonist pharmacophore. The pharmacophore features in the three-point pharmacophore are the two hydrophobic points colored green and one anionic group colored in red. The distances among the three-points are 12–16 Å and 8–14 Å from the anionic to the two hydrophobic points, and 7–12 Å between hydrophobic points.

Table 2. Pharmacophore hits obtained using different anionic isosteres in pharmacophore searches of the NCI database

Anionic group	Number of hits	Number docked in LPA_3
Phosphate	58	21
Carboxylate	748	121
Sulfonamide	131	15
Sulfate	15	5
Sulfite	146	50
Totals	1098	212

(Fig. 5A and Table 4). Further analysis revealed that NBAP matched the LPA_3 agonist as well as antagonist pharmacophore (Fig. 5B). This result necessitated that LPA_3 antagonist pharmacophore hits matching the pharmacophores for other LPA activities be eliminated to promote identification of more selective leads. LPA_1 antagonist and LPA_3 agonist pharmacophores were available for this additional filtering step (Table 3). Comparison to these pharmacophores produced a refined hitlist of 212 compounds.

The Developmental Therapeutics Program (DTP) at the National Cancer Institute provided samples of seven compounds for screening including: NSC47091, NSC161613, NSC18749, NSC1741, NSC48776, NSC168199 and NSC343949. Assay data for the six non-fluorescent compounds (structures in Fig. 6) provided by the DTP are reported in Table 4. Two compounds, NSC343949 and NSC48776, had no antagonist or agonist effect on LPA_{1-3}. NSC18749 was shown to be a weak agonist of LPA_{1-3}. NSC47091, NSC1741, and NSC161613, showed the predicted antagonist effect. NSC161613 was identified as being a selective partial antagonist of LPA_3 (IC_{50} 24 nM) over $LPA_{1/2/4/5}$. NSC47091 was dual antagonist for both LPA_2 and LPA_3 (IC_{50} 355 nM and 30 nM, respectively). NSC1741 was a pan-antagonist for LPA_1, LPA_2 and LPA_3 in the micromolar concentration range.

Three of the six non-fluorescent compounds provided by NCI, NSC47091, NSC1741, and NSC161613, were LPA_3 antagonists, as predicted by the in silico screening experiments. Docking simulations revealed that these leads exhibit several ionic interactions with LPA_3 residues that may be important for antagonist activity including K95, R3.28, and R7.36 (Table 5). Figure 7 shows the geometric fit of these three docked antagonists inside the LPA_3 pharmacophore. All three antagonists place anionic functional groups within or near the anionic pharmacophore sphere, but do not occupy both hydrophobic points when docked into the receptor. This failure to occupy the third point may explain the partial, rather than full, antagonism observed. All active compounds were predicted to have at least four ionic/polar interactions. In contrast, the inactive compounds were predicted to have three or fewer ionic/polar interactions.

NSC47091 acted as an antagonist at LPA_2 as well as LPA_3. The pharmacological profile of NSC47091 can be explained by two amino acid differences between LPA_1, LPA_2 and LPA_3. First, docking predicts that the ionic interaction of the carboxylate with K7.35 in

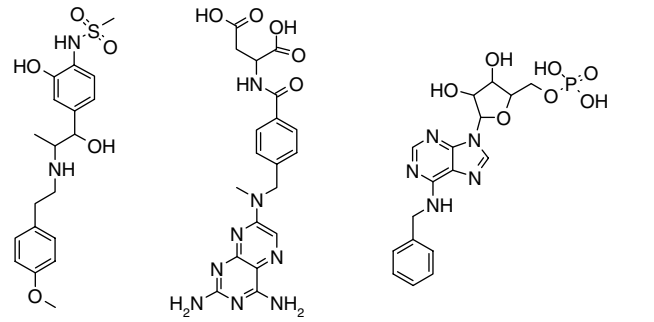

Figure 4. Representative non-lipid pharmacophore matches identified in NCI database search.

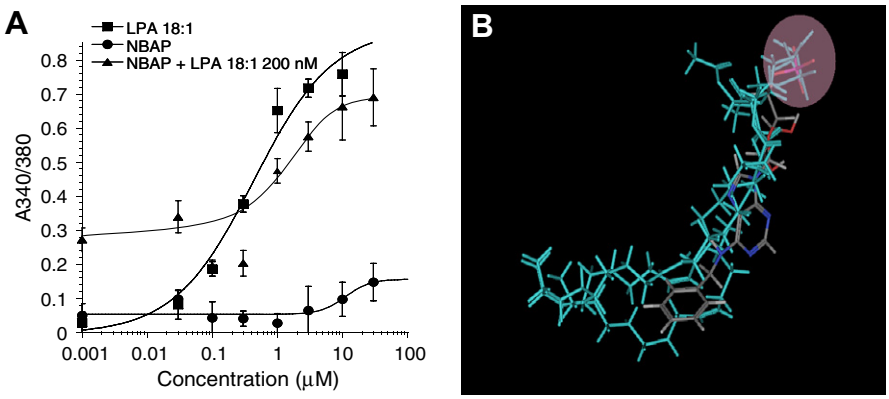

Figure 5. NBAP potentiates LPA action at LPA_3. (A) Intracellular Ca^{2+} transients (mean ± SD) were measured in response to the application of increasing concentrations of LPA 18:1 alone (filled squares), NBAP alone (filled circles), or NBAP mixed with 200 nM LPA 18:1 (filled triangles). 100% represents the maximal Ca^{2+} mobilization elicited by LPA 18:1. (B) Comparison of NBAP with docked LPA_3 agonists.[24] LPA_3 agonists are colored cyan. NBAP was flexibly aligned onto the fixed agonists showing close geometric position of anionic groups, and incomplete volume occupancy by NBAP of the bottom of the agonist binding site. The pink circle shows all phosphate groups in the same position.

Table 3. Distances between pharmacophore features derived using different LPA receptor complexes

	LPA_3 antagonist distances (Å)	LPA_1 antagonist distances (Å)	LPA_3 agonist distances (Å)
Anionic to hydrophobic	8–14 and 12–16	8–12 and 7–11	8–10 and 13–15
Hydrophobic to hydrophobic	7–12	6–10	4–5

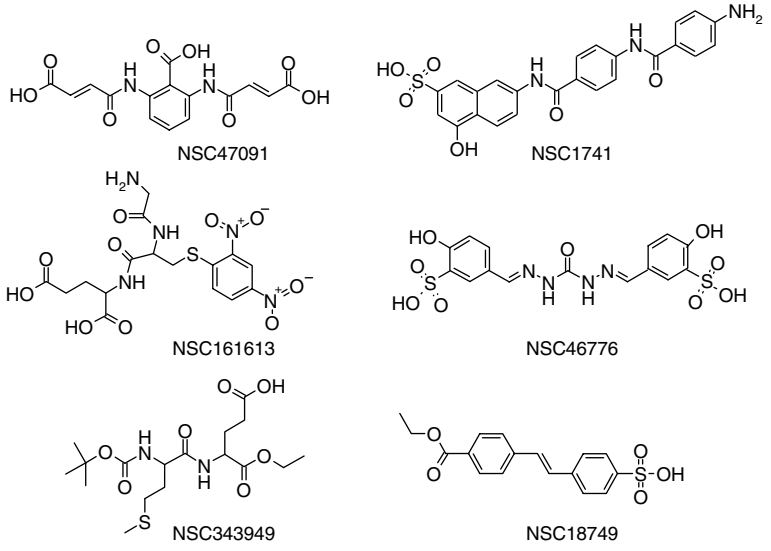

Figure 6. Compounds provided by DTP for experimental screening.

LPA_3 cannot occur in LPA_1 or LPA_2, which contain a glutamate at the corresponding site. Second, antagonist activity still occurs in LPA_2 due to an ionic interaction with H2.63, which corresponds to asparagine in the corresponding sites of LPA_1 and LPA_3.

NSC161613 was computationally and experimentally selective for LPA_3. The modeling of NSC161613 in LPA_3 showed several amino acids that might contribute to its selectivity (Fig. 8). First, an ionic interaction was observed between NSC161613 and H5. H5 corresponds to F25 in LPA_1 and Y8 in LPA_2. Second, R267 is predicted to interact with the nitro group of this compound. This interaction was lacking in both LPA_1 and LPA_2 where the R267 residue corresponds to proline and glutamate, respectively. Finally, K95 in LPA_3 is predicted to interact with the two carboxylate groups suggesting a stabilizing ionic interaction of the complex. This interaction is not present in LPA_2 where the corresponding residue is a proline.

Similarity searching using the online search tool www.hit2lead.com (ChemBridge) using NSC47091, the most efficacious antagonist, as the search target yielded 546 hits. Visual assessment ultimately reduced this number to 12 compounds that were virtually screened. Five

Table 4. Inhibition of LPA-induced calcium responses by selected NCI pharmacophore hits

Compound	LPA_1	LPA_2	LPA_3	LPA_4	LPA_5
NSC343949	No effect	No effect	No effect	NT[c]	NT[c]
NSC161613	No effect	No effect	IC_{50} 24 nM I_{max} = 69.8%[a]	No effect	No effect
NSC255523 (NBAP)	No effect	No effect	Potentiator	NT[c]	NT[c]
NSC48776	No effect	No effect	No effect	NT[c]	NT[c]
NSC1741	IC_{50} > 7.3 μM I_{max} = 59.3%[a]	IC_{50} > 9.4 μM I_{max} = 88.0%[b]	I_{max} = 53.7%[a]	NT[c]	NT[c]
NSC18749	EC_{50} > 12.3 μM E_{max} = 180 at 30 μM	EC_{50} > 11.4 μM E_{max}: 113 at 30 μM	EC_{50} > 11.8 μM E_{max}: 214 at 30 μM	NT[c]	NT[c]
NSC47091	No effect	IC_{50} 355 nM I_{max} = 53.3%[b]	IC_{50} 30 nM I_{max} = 81.7%[a]	NT[c]	NT[c]

[a] Inhibition of 200 nM LPA response.
[b] Inhibition of 10 nM LPA response.
[c] NT, not tested.

Table 5. Interaction distances between pharmacophore hits experimentally screened and LPA_3 receptor residues

Compound (LPA_3 activity)	R3.28	K7.35	R7.36	W25	K95	H5	R267	W102	Y6	Sum of ionic/polar interactions
NSC161613 (IC_{50} = 24 nM)	**1.37**		**1.27**	3.72	**1.20**	**1.72**	**1.62**	2.56	*3.57*	6
NSC47091 (IC_{50} = 30 nM)		**1.27**		3.63	**1.40**	**4.27**	**1.38**	2.64		4
NSC1741 (I_{max} = 53.7% at 200 nM)	**2.39**	*3.91*	**3.61**		*3.8*	*3.78*	*3.61*	*4.41*	*4.37*	8
NSC48776 (no effect)	**2.47**		**2.80**	3.66	**2.39**	2.79	3.33		3.56	3
NSC343949 (no effect)	*3.70*	2.81		3.87		2.50		3.54		1

Interactions with distances >4.5 Å are not included.
Ionic interactions identified by bold type.
Complementary polar interactions identified by italic type.
Hydrophobic interactions underlined.

compounds (Fig. 9) exhibiting at least four ionic/polar interactions with the LPA_3 residues identified in Table 5 were purchased and experimentally screened. Four out of the five were found to be LPA_3 antagonists with varying degrees of inhibitory effect at the other two LPA receptors (Table 6), whereas compound H2L5105099 was an $LPA_{1\&2}$ antagonist. Absence of the acid on the ring in H2L5105099 compared to NSC47091 appears to be responsible for LPA_1 antagonism and the lack of effect at LPA_3 as this compound was a potent full antagonist for both $LPA_{1\&2}$, with K_i values of 50 and 21 nM, respectively. Although H2L5186303 displayed full antagonism of LPA_{1-3}, it was more than 40- and 1800-fold more selective for LPA_2 than either LPA_3 or LPA_1.

3. Discussion

In the present study we describe the usefulness of a structure-based pharmacophore for identifying new structural classes of LPA_3 antagonists. Previous LPA_3 antagonist discoveries utilized either SAR studies of LPA analogs or high-throughput screening produced predominantly lipid antagonist classes.[15,20,30] SAR studies used an anionic head group, linker atom, and a bulky alkyl group as design features.[20,30] Our study used docking to generate a pharmacophore hypothesis which took into account the predicted interactions of the ligand and the receptor.

The NCI database is the largest freely available three-dimensional chemical database. It consists of over 250,000 compounds of which 200,000 are not found in any other database.[31] Conformations for the 250,000 compounds in the NCI database were generated using Catalyst. Up to 25 conformers have been generated for each compound yielding over 2 million conformers for the 250,000 compounds in the database.[32] This allows rapid searches for rigid docking candidates. Admittedly, 25 conformations is not an exhaustive set for flexible molecules. Incomplete representation of the conformational space of flexible molecules will result in failure to identify some flexible molecules as hits that are able to adopt conformations matching our pharmacophore. This result is acceptable as highly flexible molecules are likely to exhibit poor selectivity against the LPA receptor subtypes.

We used this database to begin identifying novel leads as potential antagonists of LPA_3. The database search utilized both geometric and physicochemical query terms. A log *P* range between two and negative two was used to reduce the number of lipid hits.[33] Virtual screening using rigid docking allowed us to rapidly screen the hits for their steric and electrostatic complementarity to the receptor. Compounds were then prioritized for pharmacological assay. This approach provided a good approximation of the bioactive conformation for LPA_3 antagonists. In another study, an EDG receptor pharmacophore for $S1P_3$ antagonism was derived without receptor structural input, resulting in 307 possible pharmacophores.[34] Application of a filtering method reduced this set to seven pharmacophore hypotheses, which produced 3 compounds active at low micromolar concentration out of 36 compounds experimentally screened.

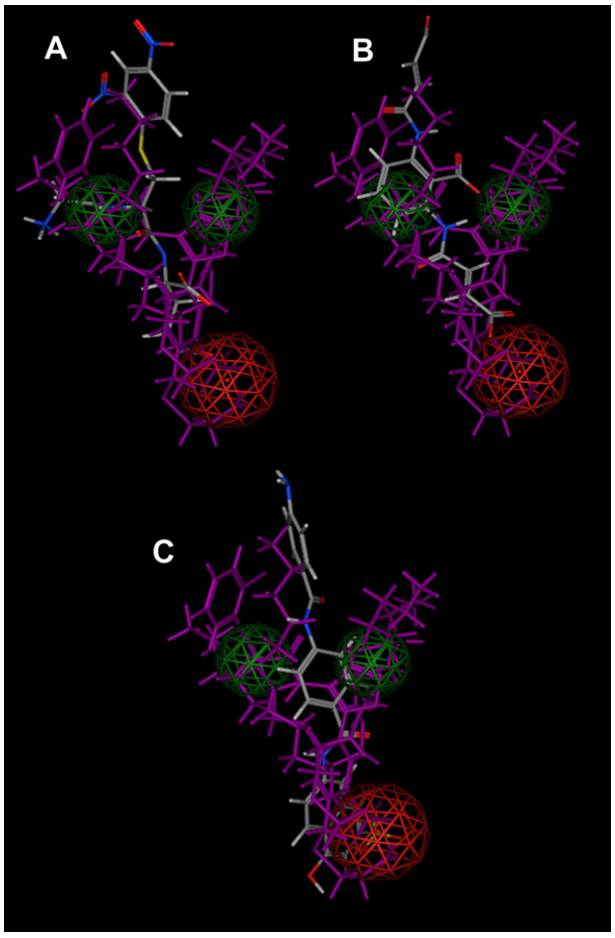

Figure 7. Confirmed antagonists identified in pharmacophore searches of the NCI database, NSC161613(A), NSC47091(B), and NSC1741(C) shown superposed on the LPA_3 antagonist pharmacophore. The three antagonists used for pharmacophore development are shown in purple along with the anionic and hydrophobic pharmacophore points in red and green, respectively.

Using hits uniquely fit to our single pharmacophore hypothesis of LPA_3 antagonism and not matching the LPA_1 antagonist or LPA_3 agonist pharmacophores, we were able to find compounds with no detectable antagonism at LPA_1 that were both non-lipid and more potent than previously described LPA_3 antagonists after screening only seven compounds. The most efficacious compound, NSC47091, was used in similarity searching. Analogs identified by similarity searching can be used to better outline pharmacophore features needed. Five non-lipid LPA_3 antagonists and a full antagonist selective for $LPA_{1\&2}$ were identified.

Using a three-point pharmacophore, we were able to identify three non-lipid LPA_3 receptor antagonists. NSC47091, NSC1741, and NSC161613 are all distinctly different from the antagonists used for the pharmacophore development and previously reported antagonists. NSC47091 and NSC161613 showed IC_{50} values of 30 nM and 24 nM, respectively, competing against 200 nM LPA 18:1 at LPA_3. Both compounds are more potent than previously reported antagonists, which showed IC_{50} values ranging from 175 to 9260 nM competing against 10 μM LPA.[18,20,27,30] In our hands, three

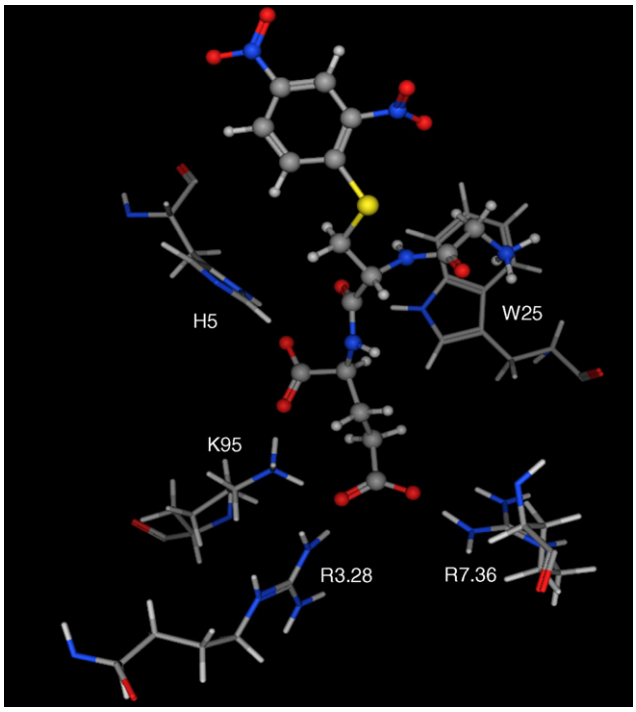

Figure 8. Key interactions observed in the NSC161613 (ball and stick) complex with LPA_3 (selected residues labeled and shown as stick models).

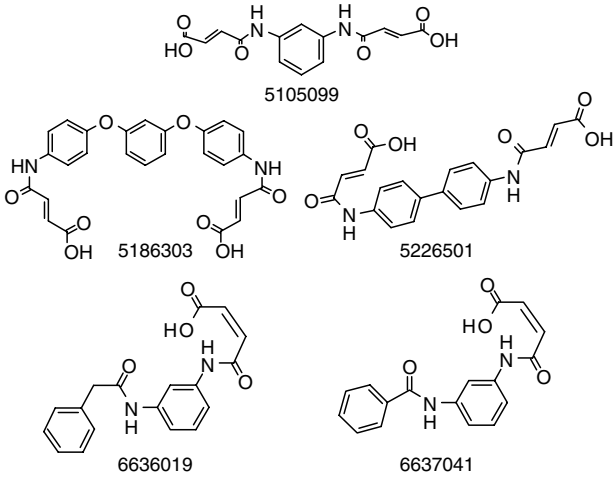

Figure 9. Similarity matches based on NSC47091 purchased from Hit2lead for experimental screening.

previously published antagonists, DGPP, Ki16425, and VPC12249 show LPA_3 K_i values of 202 nM, 148 nM, and 588 nM, respectively. NSC47091 and NSC161613 showed no antagonist activity for LPA_1, making them unique among currently known LPA_3 antagonists, which all demonstrate some antagonism of LPA_1. NSC47091 is the first reported dual antagonist of LPA_2 and LPA_3. NSC161613 was notably the first reported completely selective antagonist for LPA_3 over $LPA_{1/2/4/5}$.

One unexpected finding from this research was the novel LPA_3 potentiator, NBAP (Fig. 4). This is the first report of an allosteric regulator of LPA_3. While it is possible

Table 6. Pharmacological profiles of hit2lead compounds screened based on similarity to NSC47091

Compound	LPA_1	LPA_2	LPA_3	LPA_4	LPA_5
5105099	IC_{50} = 220 nM[a] K_i = 50 nM	IC_{50} = 21.8 nM K_i = 20.8 nM	No effect	NT[c]	NT
6637041	I_{max}= 34.6%[a] at 30μM	I_{max} = 46.0%[b] at 30 μM	IC_{50} = 347 nM K_i = 316.6 nM	NT	NT
5226501	I_{max} = 59.0%[a] at 30 μM	IC_{50} = 28.3 nM K_i = 21.1 nM	IC_{50} = 13850 nM K_i = 7020 nM	NT	NT
5186303	IC_{50} = 27354 nM K_i = 13470 nM	IC_{50} = 8.9 nM K_i = 7.2 nM	IC_{50} = 1230 nM K_i = 310 nM	NT	NT
6636019	I_{max} = 52.2%[a] at 30 μM	No effect	I_{max} = 16.0%[a] at 30 μM	NT	NT

[a] Inhibition of 200 nM LPA response.
[b] Inhibition of 25 nM LPA response.
[c] NT, not tested.

that the allosteric site is found within a single LPA_3 receptor monomer, the excellent fit of NBAP onto docked LPA_3 receptor agonists (Fig. 5B) suggests that the allosteric site might be an orthosteric site (the site responsible for agonist recognition) in the second monomer in a dimer, as reviewed by Springael et al.[35] This possibility is particularly compelling in light of the finding that LPA_3 formed homodimers in a lacZ complementation assay.[41]

Single reference similarity searching was done in an attempt to find analogs of an antagonist identified in our pharmacophore search. NSC47091 was chosen as the reference compound because it had the greatest inhibition efficacy (I_{max} = 82%) in comparison to the other two compounds identified (I_{max} < 70%). Modeling of NSC47091 and LPA_3 suggested that the anionic group on the ring was important for antagonist activity, due an ionic interaction with K7.35 in the receptor. By exploring the effects of the removal of the anionic group on the ring, we found that the anionic group was needed for LPA_3 selectivity. Figure 10A shows an overlay of NSC47091 and H2L5105099 indicating that both compounds dock in similar positions. Figure 10B shows that the most potent non-selective antagonist found (H2L518603, LPA_3 K_i = 310 nM) in similarity searching places an electronegative group in a similar position as the carboxylate group of NSC47091. This substitution is sufficient for LPA_3 antagonism, but does not lead to selectivity. These considerations suggest that in order to eliminate the LPA_1 antagonist effect, a central anionic group is required.

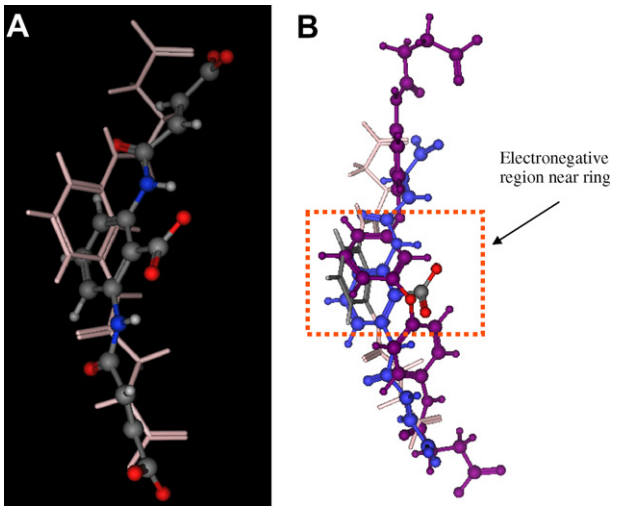

Figure 10. Superimposition of docked LPA_3 antagonist structures. (A) Superimposition of NSC47091 (ball and stick) and H2L5105099 (pink). Lack of LPA_3 activity is attributed to missing electronegative region in H2L5105099. (B) Overlay of NSC47091 (ball and stick, blue), H2L5186303 (ball and stick, purple), and H2L5105099 (stick, pink). Highlighted in the overlay is the electronegative core required for antagonist activity.

4. Conclusion

In summary, we have identified nine antagonists of LPA-elicited calcium mobilization using RH7777 cells individually expressing each of the EDG-family LPA receptors. One of these, NSC161613, is the first reported selective LPA_3 receptor antagonist. It is a potent antagonist selective for the LPA_3 receptor with no detectable activity at $LPA_{1/2/4/5}$. Another compound, H2L5186303, shows a 40- to 1800-fold selectivity for the LPA_2 receptor over $LPA_{1/3}$ with a 7.2 nM K_i. The five antagonists found by similarity searching provided data to refine the LPA_3 antagonist pharmacophore to include a fourth point promoting LPA_3 selectivity. This could not have been previously recognized based on the previous known non-selective LPA_3 antagonists. The combination of our pharmacophore model and in silico screening strategy functions as an efficient tool for identifying novel leads for the LPA_3 receptor. Efforts are ongoing to identify additional antagonists and to optimize leads using other computational methods.

5. Methods

5.1. Pharmacophore design

The pharmacophore was developed from the structure-based superposition of three known LPA_3 antagonists, the lipid-like DGP, DGTP, and non-lipid Ki16425.

The three known antagonists were built in the MOE[36] molecular modeling software package. Each of the antagonists was modeled in the ionization state expected at pH 7 and partial charges were assigned using MMFF94.[37] The antagonists were then individually flexibly docked using Autodock 3.0[38] inside the inactive LPA_3 receptor model.[23] The inactive LPA_3 receptor model, as previously described[23] is a homology model based on a crystal structure of the dark-adapted bovine rhodopsin.[39] Autodock 3.0 was used to identify the receptor-bound conformations of each antagonist. Default parameters of Autodock 3.0 were used with the following exceptions: energy evaluations (9×10^{10}), genetic algorithm search generations (3×10^4), maximum local search iterations (3×10^3), and runs (15). The docking box dimensions were 21.375 Å × 21.375 Å × 34.875 Å, with the long dimension following a line from the top of TM1 to TM4. The box was centered to include residues R276, K275, I173, L86, R105, W102, C171, N172 N89, and T90. Fifteen complexes of each antagonist were generated. The lowest docked energy complex of each antagonist was then minimized using the MMFF94[37] forcefield. In MOE[36] the individual complexes were superimposed on each other and residues within 4.5 Å of the ligands were analyzed for common ligand interactions amongst the complexes. A three-point pharmacophore hypothesis was derived consisting of two hydrophobic regions and one anionic region based on common volume occupied and receptor interactions. The distances between these points were measured to mine databases for compounds matching these dimensions.

5.2. Mining the NCI database

The distances derived from the pharmacophore hypothesis were used to search the NCI database. The database query consisted of two filters: (1) The antagonist pharmacophore hypothesis and (2) $\log P$ range between −2 and 2 to minimize the number of lipids given as hits. Multiple anionic groups were utilized including phosphate, carboxylate, sulfate, and sulfonamide.

5.3. Compound selection

The hits generated from the LPA_3 antagonist pharmacophore were further filtered by crossing these hits with the hits generated from the LPA_1 antagonist and LPA_3 agonist pharmacophores to be reported elsewhere. The conformation of each hit matching the LPA_3 antagonist pharmacophore was downloaded as a SYBYL mol2[40] format file from the NCI database.

The hits were then rigidly docked in the inactive LPA_3 receptor model using Autodock 3.0. Compounds were docked as before with the exception that 5000 generations instead of 30,000 were sufficient to obtain convergence for rigid ligands. The lowest energy receptor:ligand complex of each hit was then analyzed for intermolecular interactions within 4.5 .

A qualitative assessment comparing the docked hits of the NCI database to those used for pharmacophore development was done to select compounds for experimental testing. Priority for experimental evaluation was assigned by identifying the compounds that exhibited interactions at amino acid residues seen in complexes of the known antagonists, particularly those also required for agonist binding, and additional interactions at other amino acid residues.

5.4. Similarity searching

Similarity searching was performed using the ChemBridge online database, www.hit2lead.com. Leads experimentally confirmed as antagonists selected using pharmacophore screening were used as search target compounds. The similarity threshold was set at 60%. Compounds were visually assessed to determine how closely the structure mimicked the reference compound. Filtered hits were then flexibly docked into the inactive $LPA_{2\&3}$ receptor models. Ligand/receptor interactions were assessed and compounds were selected for biological screening using the criteria defined in Section 5.3.

5.5. Synthesis

All reagents were purchased from Sigma–Aldrich Chemical Company and Toronto Research Chemicals and were of the highest available purity. The purity of all reagents was verified by ^{1}H NMR. All ^{1}H NMR spectra were recorded on a JEOL 270-MHz spectrometer. Chemical shifts are expressed in parts per million (ppm) downfield from an internal tetramethylsilane standard. Electrospray mass spectrometric data $[M-H]^-$ was collected on a ThermoFinnigan LCQ Advantage LC–MS in the negative ion mode by direct infusion of 20 ng/μL methanol solutions.

5.5.1. Synthesis of isopropylidene protected *N*-benzyladenosine (1). To a magnetically stirred solution of *N*-benzyladenosine (500 mg, 1.40 mmol) in anhydrous acetone (150 mL) was added *p*-toluenesulfonic acid monohydrate (2.4 g, 14 mmol). The resultant pale yellow solution was maintained in an anhydrous, room temperature environment. At 15 min intervals, an aliquot of the acidic reaction mixture was removed, neutralized with a small excess of 0.5 M sodium bicarbonate solution, and analyzed via thin-layer chromatography (TLC, solvent system: 85% aqueous ethanol solution). After 45 min, the conversion of *N*-benzyl adenosine ($R_f = 0.65$) to the isopropylidene derivative ($R_f = 0.82$) was complete. The pale yellow solution was subsequently mixed with 175 mL of 0.5 M sodium bicarbonate solution and dried in vacuo, yielding 0.495 g of a white solid (89% yield). ^{1}H NMR (isopropylidene environments are in bold): **1.33 (s, 3H), 1.52 (s, 3H),** 3.53 (s, 1H), 3.42 (s, 1H), 4.11 (d, 1H), 4.14 (d, 1H), 4.18 (d, 1H), 4.22 (d, 1H), 4.71 (s, 2H), 4.86 (d, 1H), 5.36 (s, 1H), 6.14 (d, 1H), 7.27 (m, 5H), 7.41 (s, 1H), 8.23 (s, 1H), 8.46 (s, 1H).

5.5.2. Synthesis of protected *N*-benzyladenosine phosphate (2). To a stirred solution of 1 (495 mg, 1.25 mmol) in 30 mL of anhydrous dichloromethane was added di-*tert*-butyl-*N*,*N*-diisopropylphosphoramidite (750 mg,

2 mmol) and ^{1}H-tetrazole (275 mg, 4 mmol). The reaction mixture was allowed to stir for 1 h under an inert nitrogen environment at room temperature. The reaction mixture was then cooled to 0 °C and 0.3 mL of 30% hydrogen peroxide was added, and the resulting solution was stirred for 1 h. The mixture was diluted with 50 mL of dichloromethane, washed with 10% sodium metabisulfite (2× 25 mL), saturated sodium bicarbonate (2× 25 mL), water (2× 25 mL), and brine (25 mL). The organic layer was washed over anhydrous magnesium sulfate, filtered and concentrated in vacuo to yield a crude oil (313 mg, 53% yield). The resulting crude product was purified by column chromatography (60% hexane 40% ethyl acetate solvent system) to elute the desired protected phosphate 2 (212 mg, 36% yield from compound **1**) as a clear oil. ^{1}H NMR (*tert*-butyl resonance is in bold): **1.27 (s, 18H),** 1.33 (s, 3H), 1.52 (s, 3H), 3.53 (s, 1H), 3.42 (s, 1H), 4.11 (d, 1H), 4.14 (d, 1H), 4.18 (d, 1H), 4.22 (d, 1H), 4.71 (s, 2H), 4.86 (d, 1H), 6.14 (d, 1H), 7.27 (m, 5H), 7.41 (s, 1H), 8.23 (s, 1H), 8.46 (s, 1H).

5.5.3. Synthesis of *N*-benzyladenosine phosphate (3). To a stirred solution of **2** (212 mg, 0.36 mmol) in 50 mL of anhydrous dicholoromethane was added trifluoroacetic acid (0.6 mL, 8.7 mmol) and deionized water (36 μL, 2 mmol). The resulting mixture was allowed to stir at room temperature for 5 h and reaction completion was verified via TLC. Solvents were removed in vacuo and the residue was washed with dichloromethane (2× 40 mL). Concentration in vacuo yielded **3** as a colorless oil (103 mg, 61% yield from **2**). ^{1}H NMR 3.53 (s, 1H), 3.42 (s, 1H), 4.11 (d, 1H), 4.14 (d, 1H), 4.18 (d, 1H), 4.22 (d, 1H), 4.71 (s, 2H), 4.86 (d, 1H), 6.14 (d, 1H), 7.27 (m, 5H), 7.41 (s, 1H), 8.23 (s, 1H), 8.46 (s, 1H). MS: $[M-H]^-$ at *m*/*z* 476.

5.6. Measurement of intracellular Ca^{2+} mobilization

The rat hepatoma (RH7777) cell lines individually expressing either LPA_1, LPA_2, LPA_3 or LPA_5 receptors and the Chinese hamster ovary (CHO) cell line expressing LPA_4 were analyzed to examine agonism and antagonism. Wild type RH7777 cells do not respond to LPA with changes in $[Ca^{2+}]_i$. CHO cells stably expressing either vector or LPA_4 were a kind gift from Dr. Shimizu (University of Tokyo, Tokyo, Japan).

Stable transformants of $LPA_{1/2/3}$ receptors: RH7777 cells stably expressing each receptor were plated onto poly-L-lysine (PLL, 0.1 mg/mL)-coated black-wall clear-bottom 96-well plates (Corning Incorporated Life Sciences, Acton, MA) at a density of 5×10^4 cells/well and cultured overnight. The following day, the culture medium was replaced with modified Krebs buffer (120 mM NaCl, 5 mM KCl, 0.62 mM $MgSO_4$, 1.8 mM $CaCl_2$, 10 mM Hepes, 6 mM glucose, pH 7.4), and the cells were serum starved for 6 h. Subsequently, cells were loaded with Fura-2 AM (Invitrogen, Carlsbad, CA) for 35 min in modified Krebs buffer containing 2% (v/v) pluronic acid.

Stable transformants of LPA_4: CHO cells stably expressing either vector or LPA_4 were plated onto non-coated 96-well plates at a density of 4×10^4 cells/well and cultured overnight. The following day, cells were loaded with Fura-2 AM for 1 h in modified Krebs buffer containing 2% (v/v) pluronic acid and 2.5 mM probenecid.

Transient transfection of LPA_5: RH7777 cells in 10 cm dish at a density of 2×10^6 were transfected with 2 μg of plasmid DNA with Effectene (Qiagen, Valencia, CA) according to the manufacturer's instructions for 24 h, then replated onto PLL-coated 96-well plates at a density of 5×10^4 cells/well and cultured overnight. The following day, the culture medium was replaced with modified Krebs buffer, and the cells were serum starved for 4 h. Cells were loaded with Fura-2 AM for 30 min in modified Krebs buffer containing 2% (v/v) pluronic acid.

After incubating the cells with Fura-2 AM, the cells were rinsed with Krebs buffer and changes in the intracellular Ca^{2+} concentration were monitored by determining the ratio of emitted light intensities at 520 nm in response to excitation at 340 and 380 nm using a FLEXstation II (Molecular Devices, Sunnyvale, CA). Each well was monitored for 80–120 s. For testing agonist activity of the compounds, the test compounds were added automatically after 15 s of baseline measurement. To determine antagonist properties, varying concentrations of the compounds were mixed with constant concentration of LPA and responses were monitored. Each test was performed in quadruplicate. CHO cells endogenously express LPA_1, therefore, to access the effect of LPA_4 in CHO cells, the response in vector-transfected cells was subtracted from the response in LPA_4-transfected cells.

One hit, NSC168199, showed strong fluorescence that interfered with the Ca^{2+} assay. Fluorescence of the compounds was determined by dissolving 10 μM of each compound into 100 μL Krebs buffer per well and measuring autofluorescence to excitation at 340 and 380 nm using a FLEXstation II (Molecular Devices, Sunnyvale, CA). NSC168199 was excluded from further testing due to autofluorescence.

5.7. Statistical analysis

Significant difference was determined by the Student's test at a P value of 0.05. IC_{50} values were calculated by fitting a sigmoid function to data points by using the non-linear curve-fitting feature of KaleidaGraph (Synergy Software, Essex Junction, VT).

Acknowledgments

This work was supported by grants from the National Institutes of Health (RO1 HL84007 to A.P. and RO1 CA92160 to G.T.). This work was supported by awards from the Greater Southeast Affiliate of the American Heart Association (0715125B to J.F., 0625325B to Y.F. and 0725528B to D.O.). The MOE program was donated by the Chemical Computing Group and is greatly appreciated. A special thanks to the NCI Developmental Therapeutics Program (DTP) for freely providing compounds for experimental validation.

References and notes

1. Mills, G. B.; Moolenaar, W. H. *Nat. Rev. Cancer* **2003**, *3*, 582–591.
2. Tigyi, G.; Parrill, A. L. *Prog. Lipid Res.* **2003**, *42*, 498–526.
3. Anliker, B.; Chun, J. *J. Biol. Chem.* **2004**, *279*, 20555–20558.
4. Noguchi, K.; Ishii, S.; Shimizu, T. *J. Biol. Chem.* **2003**, *278*, 25600–25606.
5. Kotarsky, K.; Boketoft, A.; Bristulf, J.; Nilsson, N.; Norberg, A.; Hansson, S.; Sillard, R.; Owman, C.; Leeb-Lundberg, F.; Olde, B. *J. Pharmacol. Exp. Ther.* **2006**.
6. Tabata, K.; Baba, K.; Shiraishi, A.; Ito, M.; Fujita, N. *Biochem. Biophys. Res. Commun.* **2007**, *363*, 861–866.
7. Rizza, C.; Leitinger, N.; Yue, J.; Fischer, D. J.; Wang, D. A.; Shih, P. T.; Lee, H.; Tigyi, G.; Berliner, J. A. *Lab. Invest.* **1999**, *79*, 1227–1235.
8. Zhang, C.; Baker, D. L.; Yasuda, S.; Makarova, N.; Balazs, L.; Johnson, L. R.; Marathe, G. K.; McIntyre, T. M.; Xu, Y.; Prestwich, G. D.; Byun, H. S.; Bittman, R.; Tigyi, G. *J. Exp. Med.* **2004**, *199*, 763–774.
9. Deng, W.; Shuyu, E.; Tsukahara, R.; Valentine, W. J.; Durgam, G.; Gududuru, V.; Balazs, L.; Manickam, V.; Arsura, M.; VanMiddlesworth, L.; Johnson, L. R.; Parrill, A. L.; Miller, D. D.; Tigyi, G. *Gastroenterology* **2007**, *132*, 1834–1851.
10. Pilquil, C.; Dewald, J.; Cherney, A.; Gorshkova, I.; Tigyi, G.; English, D.; Natarajan, V.; Brindley, D. N. *J. Biol. Chem.* **2006**, *281*, 38418–38429.
11. Takuwa, Y.; Takuwa, N.; Sugimoto, N. *J. Biochem. (Tokyo)* **2002**, *131*, 767–771.
12. Contos, J. J. A.; Ishii, I.; Chun, J. *Mol. Pharmacol.* **2000**, *58*, 1188–1196.
13. Bandoh, K.; Aoki, J.; Hosono, H.; Kobayashi, S.; Kobayashi, T.; Murakami-Murofushi, K.; Tsujimoto, M.; Arai, H.; Inoue, K. *J. Biol. Chem.* **1999**, *274*, 27776–27785.
14. Ye, X.; Hama, K.; Contos, J. J. A.; Anliker, B.; Inoue, A.; Skinner, M. K.; Suzuki, H.; Amano, T.; Kennedy, G.; Arai, H.; Aoki, J.; Chun, J. *Nature* **2005**, *435*, 104–108.
15. Ohta, H.; Sato, K.; Murata, D. A.; Damirin, A.; Malchinkhuu, E.; Kon, J.; Kimura, T.; Tobo, M.; Yamazaki, Y.; Watanabe, T.; Yagi, M.; Sato, M.; Suzuki, R.; Murooka, H.; Saka, T.; Nishitoba, T.; Im, D. S.; Nochi, H.; Tamoto, K.; Tomura, H.; Okajima, F. *Mol. Pharmacol.* **2003**, *64*, 994–1005.
16. Fukushima, N.; Chun, J. *Prost. Lipid Mediators* **2001**, *64*, 21–32.
17. Durgam, G. G.; Tsukahara, R.; Makarova, N.; Walker, M. D.; Fujiwara, Y.; Pigg, K. R.; Baker, D. L.; Sardar, V. M.; Parrill, A. L.; Tigyi, G.; Miller, D. D. *Bioorg. Med. Chem. Lett.* **2006**, *16*, 633–640.
18. Virag, T.; Elrod, D. B.; Liliom, K.; Sardar, V. M.; Parrill, A. L.; Yokoyama, K.; Durgam, G.; Deng, W.; Miller, D. D.; Tigyi, G. *Mol. Pharmacol.* **2003**, *63*, 1032–1042.
19. Santos, W. L.; Heasley, B. H.; Jarosz, R.; Carter, K. M.; Lynch, K. R.; Macdonald, T. L. *Bioorg. Med. Chem. Lett.* **2004**, *14*, 3473–3476.
20. Heasley, B. H.; Jarosz, R.; Lynch, K. R.; Macdonald, T. L. *Bioorg. Med. Chem. Lett.* **2004**, *14*, 2735–2740.
21. Fujiwara, Y.; Sardar, V. M.; Tokumura, A.; Baker, D. L.; Murakami-Murofushi, K.; Parrill, A. L.; Tigyi, G. *J. Biol. Chem.* **2005**, *280*, 35038–35050.
22. Parrill, A. L.; Sardar, V. M.; Yuan, H. *Sem. Cell Dev. Biol.* **2004**, *15*, 467–476.
23. Sardar, V. M.; Bautista, D. L.; Fisher, D. J.; Yokoyama, K.; Nusser, N.; Virag, T.; Wang, D.; Baker, D. L.; Tigyi, G.; Parrill, A. L. *Biochim. Biophys. Acta* **2002**, *1582*, 309–317.
24. Fujiwara, Y.; Osborne, D. A.; Walker, M. D.; Wang, D.-a.; Bautista, D. A.; Liliom, K.; Van Brocklyn, J. R.; Parrill, A. L.; Tigyi, G. *J. Biol. Chem.* **2007**, *282*, 2374–2385.
25. Ballesteros, J. A.; Weinstein, H. *Methods Neurosci.* **1995**, *25*, 366–425.
26. Parrill, A. L.; Baker, D. L.; Wang, D.; Fischer, D. J.; Bautista, D., et al. *NY Acad. Sci.* **2000**, 330–339.
27. Fischer, D. J.; Nusser, N.; Virag, T.; Yokoyama, K.; Wang, D.; Baker, D. L.; Bautista, D.; Parrill, A. L.; Tigyi, G. *Mol. Pharmacol.* **2001**, *60*, 776–784.
28. Lynch, K. R.; Macdonald, T. L. *Biochim. Biophys. Acta* **2002**, *1582*, 289–294.
29. Milne, G. W. A.; Nicklaus, M. C.; Driscoll, J. S.; Wang, S.; Zaharevitz, D. *J. Chem. Inf. Comp. Sci.* **1994**, *34*, 1219–1224.
30. Heasley, B. H.; Jarosz, R.; Carter, K. M.; Jenny Van, S.; Lynch, K. R.; Macdonald, T. L. *Bioorg. Med. Chem. Lett.* **2004**, *14*, 4069–4074.
31. Voigt, J. H.; Bienfait, B.; Wang, S.; Nicklaus, M. C. *J. Chem. Inf. Comput. Sci.* **2001**, *41*, 702–712.
32. Ihlenfeldt, W.-D.; Voigt, J. H.; Bienfait, B.; Oellien, F.; Nicklaus, M. C. *J. Chem. Inf. Comput. Sci.* **2002**, *42*, 46–57.
33. Avdeef, A. *Curr. Top. Med. Chem.* **2001**, *1*, 277–351.
34. Koide, Y.; Uemoto, K.; Hasegawa, T.; Sada, T.; Murakami, A.; Takasugi, H.; Sakurai, A.; Mochizuki, N.; Takahashi, A.; Nishida, A. *J. Med. Chem.* **2007**, *50*, 442–454.
35. Springael, J.-Y.; Urizar, E.; Costagliola, S.; Vassart, G.; Parmentier, M. *Pharm. Ther.* **2007**, *115*, 410–418.
36. MOE; 2004.03 ed.; Chemical Computing Group: Montreal.
37. Halgren, T. A. *J. Comput. Chem.* **1996**, *17*, 490–519.
38. Morris, G. M.; Goodsell, D. S.; Halliday, R. S.; Huey, R.; Hart, W. E.; Belew, R. K.; Olson, A. J. *J. Comput. Chem.* **1998**, *19*, 1639–1662.
39. Palczewski, K.; Kumasaka, T.; Hori, T.; Behnke, C. A.; Motoshima, H.; Fox, B. A.; Le Trong, I.; Teller, D. C.; Okada, T.; Stenkamp, R.; Yamamoto, M.; Miyano, M. *Science* **2000**, *289*, 739–745.
40. SYBYL Mol2 file format; Tripos, Inc.: USA.
41. Zaslavsky, A.; Singh, L. S.; Tan, H.; Ding, H.; Liang, Z.; Xu, Y. *Biochim. Biophys. Acta* **2006**, *1761*, 1200–1212.